

Bi-Directional Reflectance Distribution Function: BRDF Effect on Un-mixing, Category Decomposition of the Mixed Pixel (MIXEL) of Remote Sensing Satellite Imagery Data

Kohei Arai ¹

Graduate School of Science and Engineering
Saga University
Saga City, Japan

Abstract—Method for unmixing, category decomposition of the mixed pixel (MIXEL) of remote sensing satellite imagery data taking into account the effect due to Bi-Directional Reflectance Distribution Function: BRDF is proposed. Although there is not so small BRDF effect on estimation mixing ratios, conventional unmixing methods do not take into account the effect. Through experiments, the effect is clarified. Also the proposed unmixing method with consideration of BRDF effect is validated.

Keywords—Unmixing; BRDF; Mixel; Lambertian surface; Category decomposition

I. INTRODUCTION

The pixels in earth observed images which are acquired with Visible to Near Infrared: VNIR sensors onboard remote sensing satellites are, essentially mixed pixels (mixels) which consists of several ground cover materials [1]. Some mixel model is required for analysis such as un-mixing of the mixel in concern [2],[3]. Typical mixel is linear mixing model which is represented by linear combination of several ground cover materials with mixing ratio for each material [4]. It is not always true that the linear mixel model is appropriate [5]. Due to the influences from multiple reflections between the atmosphere and ground, multiple scattering in the atmosphere on the observed radiance from the ground surface, pixel mixture model is essentially non-linear rather than linear. These influences are interpreted as adjacency effect [6], [7].

Although there is not so small BRDF effect on estimation mixing ratios, conventional unmixing methods do not take into account the effect. Method for unmixing, category decomposition of the mixed pixel (MIXEL) of remote sensing satellite imagery data taking into account the effect due to Bi-Directional Reflectance Distribution Function: BRDF is proposed. In order to take into account BRDF effect, Minneart Reflectance Model: MRM is utilized for representation of BRDF. Through experiments, the effect is clarified. Also the proposed unmixing method with consideration of BRDF effect is validated.

The following section, the proposed method is described followed by the experiments. Then conclusion is described together with some discussions.

II. PROPOSED METHOD

A. Surface Reflectance Models

BRDF is defined in equation (1).

$$dL_i(\theta_i, \phi_i, \theta_r, \phi_r, E_i) / dE_i(\theta_i, \phi_i) \quad (1)$$

Where $dL_i(\theta_i, \phi_i, \theta_r, \phi_r, E_i)$ and $dE_i(\theta_i, \phi_i)$ denotes reflected radiance and incident irradiance, reflectively.

Lambertian surface, on the other hand, is defined in equation (2).

$$I_\theta = I_n \cos \theta \quad (2)$$

Where I_n denote incident irradiance in the normal direction while I_θ denotes reflected radiance in direction of θ . Therefore, the Lambertian surface reflectance is constant at all direction, for entire hemisphere.

Minneart reflection is defined in equation (3).

$$B(\gamma, \nu) = \frac{k+1}{2\pi} (\gamma\nu)^{k-1} \quad (3)$$

Where γ, ν denotes solar zenith angle and observation angle, respectively while k denotes Minneart coefficient. If $k=1$, it is totally equation to Lambertian surface.

B. Unmixing, Category Decomposition Method

One single pixel of remote sensing satellite imagery data, P can be represented as combination of weighted spectral characteristics, H_j of the considerable ground cover targets included in the Instantaneous Field of View: IFOV with their mixing ratios, a_j as is shown in equation (4).

$$P = \sum_{j=1}^k a_j H_j$$
$$\sum_{j=1}^k a_j = 1$$
$$a_j \geq 0 \quad (4)$$

This is rewritten in the following vector representation,

$$P = HA \tag{5}$$

where

$$P = [p_1, p_2, \dots, p_n]^t$$

$$H = \begin{bmatrix} h_{11} & h_{12} & \dots & h_{1k} \\ h_{21} & h_{22} & \dots & h_{2k} \\ \vdots & \vdots & \ddots & \vdots \\ h_{n1} & h_{n2} & \dots & h_{nk} \end{bmatrix}$$

$$A = [a_1, a_2, \dots, a_k]^t \tag{6}$$

In general, H is rectangle matrix. Therefore, Moore-Penrose generalized inverse matrix is needed to estimate mixing ratio vector A as shown in equation (7).

$$A = (H^t H)^{-1} H^t P$$

$$= H^+ P$$

$$H^+ = (H^t H)^{-1} H^t \tag{7}$$

C. Monte Carlo Ray Tracing Simulation

In order to show a validity of the proposed non-linear mixel model, MCRT simulation study and field experimental study is conducted. MCRT allows simulation of polarization characteristics of sea surface with designated parameters of the atmospheric conditions and sea surface and sea water conditions. Illustrative view of MCRT is shown in Figure 1.

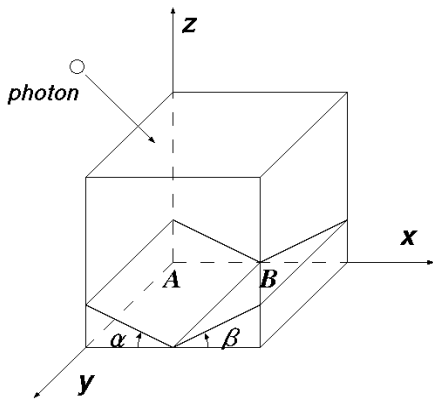


Fig. 1. Illustrative view of MCRT for the atmosphere and sea water

Photon from the sun is input from the top of the atmosphere (the top of the simulation cell). Travel length of the photon is calculated with optical depth of the atmospheric molecule and that of aerosol. There are two components in the atmosphere; molecule and aerosol particles while three are also two components, water and particles; suspended solid and phytoplankton in the ocean.

When the photon meets molecule or aerosol (the meeting probability with molecule and aerosol depends on their optical depth), then the photon scattered in accordance with scattering properties of molecule and aerosol. The scattering property is called as phase function¹. In the visible to near infrared wavelength region, the scattering by molecule is followed by Rayleigh scattering law [8] while that by aerosol is followed by Mie scattering law [8]. Example of phase function of Mie scattering is shown in Figure 2 (a) while that of Rayleigh scattering is shown in Figure 2 (b).

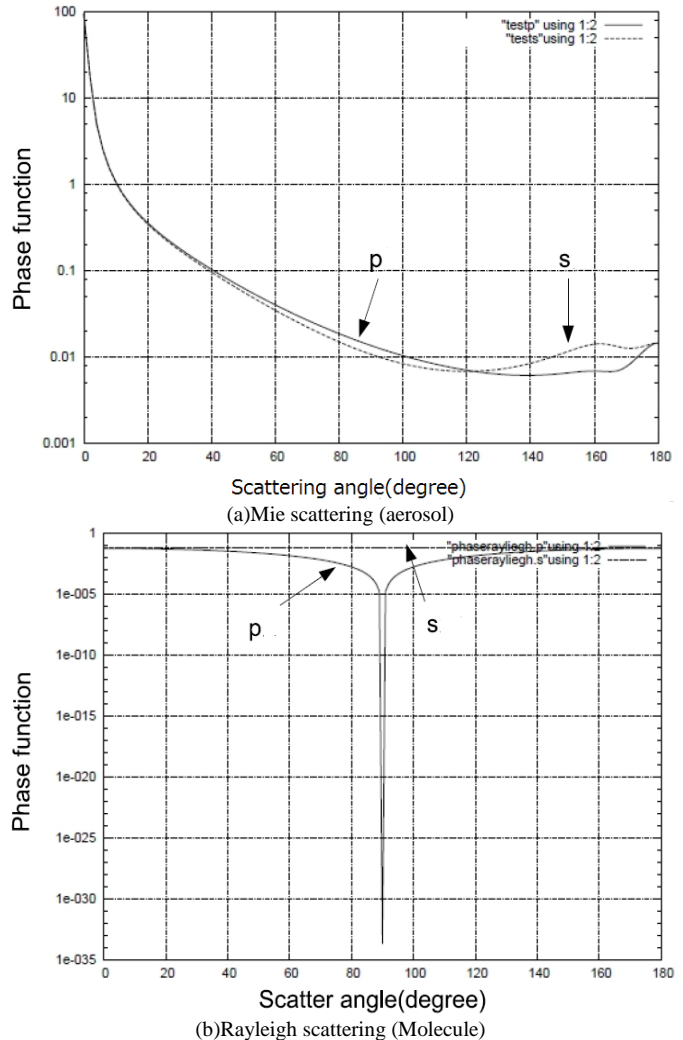


Fig. 2. Phase functions for Mie and Rayleigh scattering

In the atmosphere, there are absorption due to water vapor, ozone and aerosols together with scattering due to the atmospheric molecules, aerosols. Atmospheric Optical Depth: AOD (optical thickness) in total, Optical Depth: OD due to water vapor (H₂O), ozone (O₃), molecules (MOL), aerosols (AER), and real observed OD (OBS) are plotted in Figure 3 as an example.

¹ <http://ejje.weblio.jp/content/phase+function>

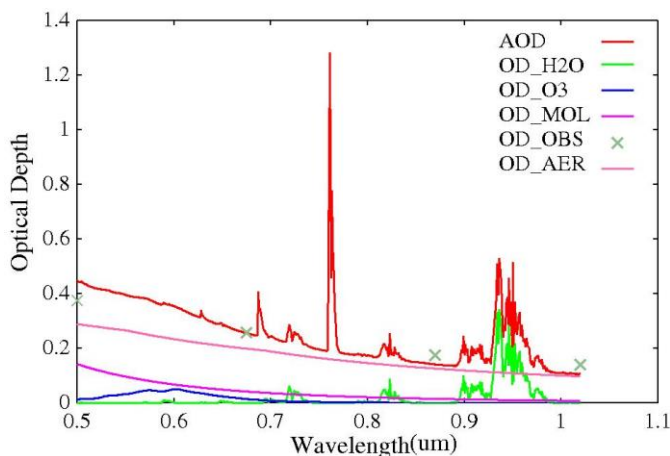


Fig. 3. Example of observed atmospheric optical depth in total and the best fit curves of optical depth due to water vapor, ozone, molecules, and aerosols calculated with MODTRAN of atmospheric radiative transfer software code..

For simplifying the calculations of the atmospheric influences, it is assumed that the atmosphere containing only molecules and aerosols. As shown in Figure 3, this assumption is not so bad. Thus the travel length of the photon at once, L is expressed with equation (8).

$$L=L_0 \text{RND}(i) \quad (8)$$

$$L_0=Z_{max}/\tau \quad (9)$$

Where Z_{max} , τ , $\text{RND}(i)$ are maximum length, altitude of the atmosphere, optical depth, and i -th random number, respectively. In this equation, τ is optical depth of molecule or aerosol. The photon meets molecule when the random number is greater than τ . Meanwhile, if the random number is less than τ , then the photon meets aerosol. The photon is scattered at the molecule or aerosol to the direction which is determined with the aforementioned phase function and with the rest of the travel length of the photon.

III. SIMULATION STUDIES AND THE EXPERIMENTS

A. Preliminary Simulation Studies

A mixed pixel model which consists of two categories is created. Also two different surface reflectance models, Minneart and Lambertian surface models are assumed as shown in Figure 4.

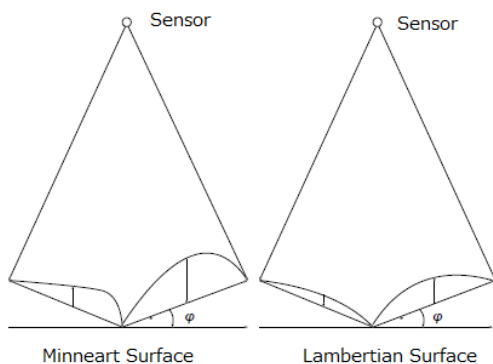


Fig. 4. Assumed surface models for simulation study

Alunite and Cheat grass are selected for the categories. These spectral characteristics are given by USGS spectral library. Mixel with 50% of Alunite and 50% of Cheat grass is created with the surface slope of 20 degree. Observed radiance from the mixel is derived from MCRT at wavelength of 550 and 650 nm. Unmixing is attempted with Minneart and Lambertian surface models. Spectral characteristics of Alunite and Cheat grass are shown in Figure 5 (a) and (b). Also angle distribution of Minneart surface with Minneart coefficients of 0.3, 0.8 and 1.0 (Lambertian surface) is shown in Figure 6. Due to the fact that the surface slope angle is set at 20 degree, reflectance between Lambertian and Minneart reflection models show no difference at 20 and 110 degree of observation angles. Also Figure 7 shows reflectance as a function of slope. Figure 7 (a) shows the calculated reflectance of Alunite as a function of slope angle with the different parameters of Minneart coefficients, 0.3, 0.8, and 1.0 while Figure 7 (b) shows that of Cheat grass as a function of slope angle with the different parameters of Minneart coefficients, 0.3, 0.8, and 1.0 at the wavelength of 550 nm. Therefore, slope effect is quite dependent on Minneart coefficients. Unmixing results based on Minneart reflectance model show correct mixing ratio of 50 versus 50% while those based on Lambert reflectance model show 52.25 versus 47.75%.

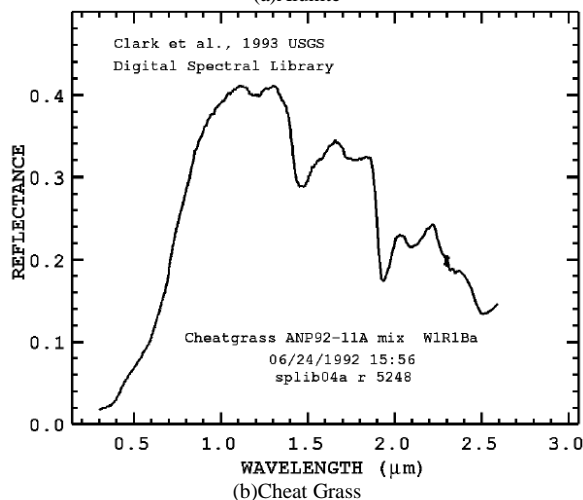
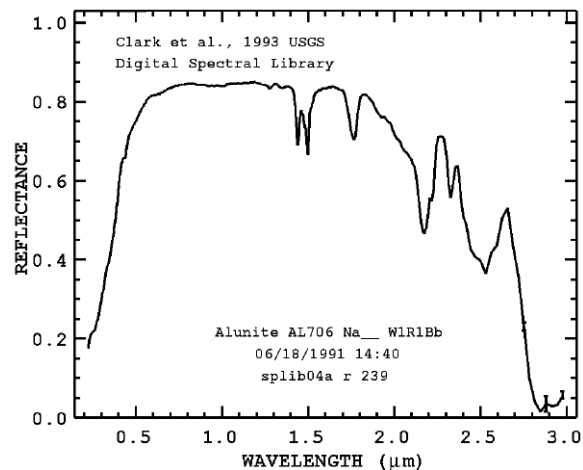


Fig. 5. Spectral characteristics of Alunite and Cheat grass derived from USGS spectral library

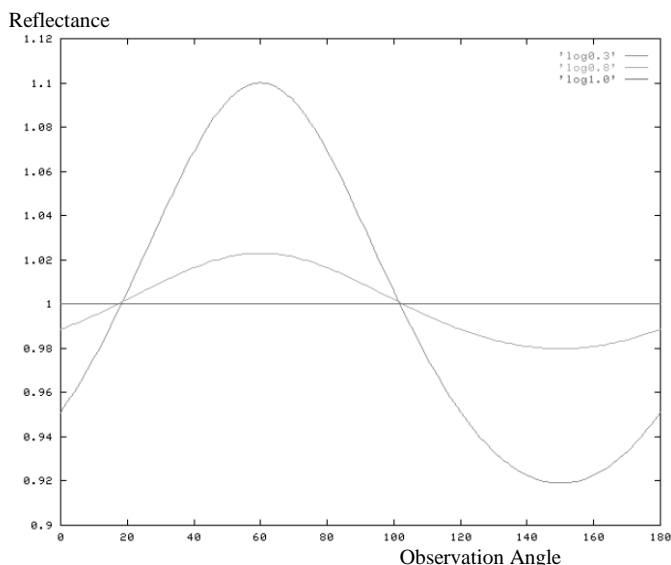
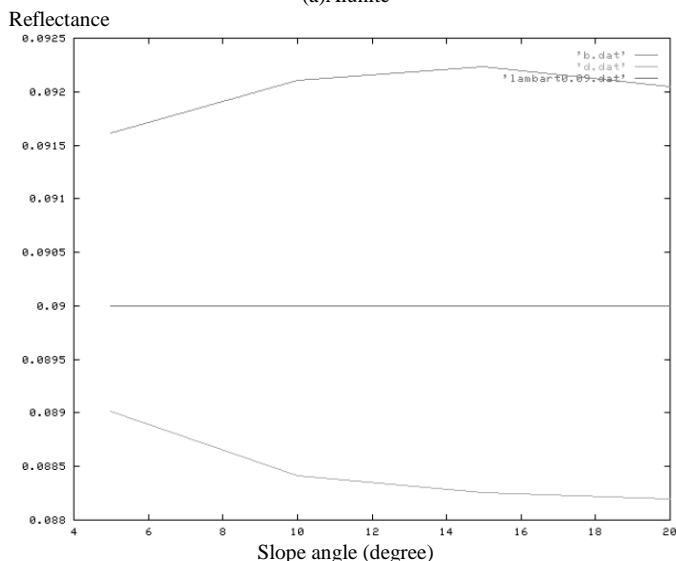
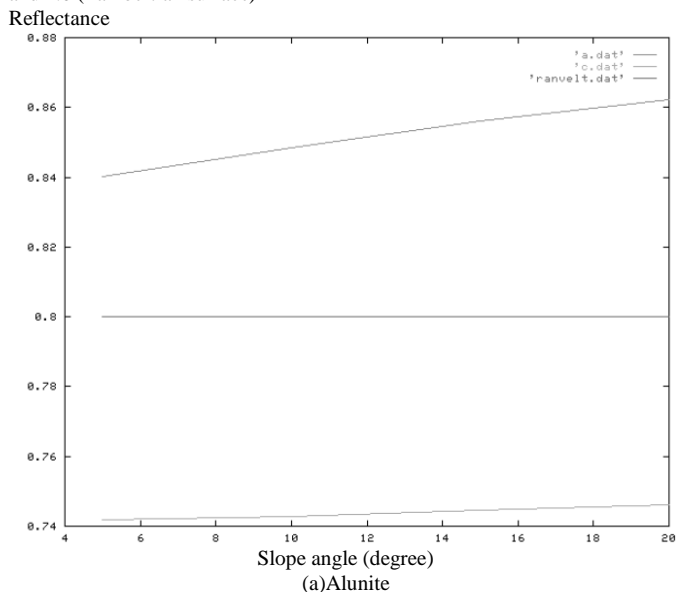


Fig. 6. Angle distribution of reflectance at Minneart coefficients, 0.3, 0.8, and 1.0 (Lambertian surface)



(b)Cheat grass
Fig. 7. Slope effect on the calculated surface reflectance

Therefore, 2.25% of estimation error is observed for the mixing ratio for the Lambertian surface model. The results show that there is significant error on mixing ratio estimation when BRDF is not taken into account.

B. Simulation Studies

Visible to Near Infrared: VNIR radiometer onboard remote sensing satellite is simulated with MCRT. VNIR consists of three bands, 400, 700, and 900nm with IFOV of 15m. Observation angle is set at zero zenith angle (nadir view) while solar zenith angle is set at 20 degree.

Ground surface is assumed to be covered with soil) default materials of MODTRAN. Within a IFOV, there are three soils with the different reflectance, 0.1, 0.3, and 0.5 of Lambertian and Minneart surfaces. Minneart coefficients are 1.0 for Lambertian surface and 0.8 for Minneart surface, respectively.

Mid. Latitude Summer of the atmospheric model is selected from MODTRAN. Optical depth of atmospheric molecule is set at 0.0003 while that of aerosol particle is set at 0.2 at 700 nm. Refractive index of aerosol particle is set at 1.44 - i 0.005. Junge size distribution of aerosol particle is assumed with Junge parameter of 3.0. Then phase function (scattering characteristic) can be derived from Mie code which is included in MODTRAN. Top of the Atmosphere: TOA radiance, then calculated for pixel by pixel basis. Table 1 shows the TOA radiance in unit of mW/cm²/str. Also the TOA radiance of the assumed mixels with the different mixing ratio is calculated. Mixing ratio of 0.1, 0.3, and 0.5 of reflectance soils is 0.5, 0.3, and 0.2, The results are 0.295 (@400nm), 0.222 (@700nm), and 0.185 (@900nm), respectively for Lambertian surface while those for Mineart surface are 0.262 (@400nm), 0.201 (@700nm), and 0.175 (@900nm), respectively.

Using the aforementioned TOA radiance of the assumed mixels for both Lambertian and Minneart surfaces, mixing ratio of the different reflectance of soils are estimated based on the proposed unmixing method of category decomposition. The result is as follows,

6.65% (soil #1), 82.74% (soil #2), 10.61% (soil #3) for Lambertian surface while
49.95% (soil #1), 27.59% (soil #2), 22.46% (soil #3) for Minneart surface.

TABLE I. TOA RADIANCE

(a) Lambertian Surface			
Reflectance	TOA radiance (mW/cm ² /str)		
	@400nm	@700nm	@900nm
0.1	0.240	0.189	0.166
0.3	0.322	0.236	0.196
0.5	0.441	0.291	0.234

(b)Minneart Surface			
Reflectance	TOA radiance (mW/cm ² /str)		
	@400nm	@700nm	@900nm
0.1	0.226	0.183	0.162
0.3	0.277	0.210	0.185
0.5	0.350	0.247	0.209

This implies that the estimated mixing ratios are appropriate when BRDF is taken into account (Minneart surface) while the estimated mixing ratios have significant errors if BRDF is not taken into account (Lambertian surface).

IV. CONCLUSION

Method for unmixing, category decomposition of the mixed pixel (MIXEL) of remote sensing satellite imagery data taking into account the effect due to Bi-Directional Reflectance Distribution Function: BRDF is proposed. Although there is not so small BRDF effect on estimation mixing ratios, conventional unmixing methods do not take into account the effect. Through experiments, the effect is clarified. Also the proposed unmixing method with consideration of BRDF effect is validated.

The estimated mixing ratios are appropriate when BRDF is taken into account (Minneart surface) while the estimated mixing ratios have significant errors if BRDF is not taken into account (Lambertian surface).

ACKNOWLEDGMENT

The author would like to thank Ms. Chiaki Sakai for his efforts through experiments and simulations.

REFERENCES

- [1] Masao Matsumoto, Hiroki Fujiku, Kiyoshi Tsuchiya, Kohei Arai, Category decomposition in the maximum likelihood classification, Journal of Japan Society of Phtogrammetro and Remote Sensing, 30, 2, 25-34, 1991.
- [2] Masao Moriyama, Yasunori Terayama, Kohei Arai, Claffication method based on the mixing ratio by means of category decomposition, Journal of Remote Sensing Society of Japan, 13, 3, 23-32, 1993.

- [3] Kohei Arai and H.Chen, Unmixing method for hyperspectral data based on subspace method with learning process, Techninical Notes of the Science and Engineering Faculty of Saga University,, 35, 1, 41-46, 2006.
- [4] Kohei Arai and Y.Terayama, Label Relaxation Using a Linear Mixture Model, International Journal of Remote Sensing, 13, 16, 3217-3227, 1992.
- [5] Kohei Arai, Yasunori Terayama, Yoko Ueda, Masao Moriyama, Cloud coverage ratio estimations within a pixel by means of category decomposition, Journal of Japan Society of Phtogrammetro and Remote Sensing, 31, 5, 4-10, 1992.
- [6] Kohei Arai, Non-linear mixture model of mixed pixels in remote sensing satellite images based on Monte Carlo simulation, Advances in Space Research, 41, 11, 1715-1723, 2008.
- [7] Kohei Arai, Kakei Chen, Category decomposition of hyper spectral data analysis based on sub-space method with learning processes, Journal of Japan Society of Phtogrammetro and Remote Sensing, 45, 5, 23-31, 2006.
- [8] Arai, K, Lecture Notes on Remote Sensing, Morikita-Shuppan, Co.Ltd., 2005

AUTHORS PROFILE

Kohei Arai, He received BS, MS and PhD degrees in 1972, 1974 and 1982, respectively. He was with The Institute for Industrial Science and Technology of the University of Tokyo from April 1974 to December 1978 also was with National Space Development Agency of Japan from January, 1979 to March, 1990. During from 1985 to 1987, he was with Canada Centre for Remote Sensing as a Post Doctoral Fellow of National Science and Engineering Research Council of Canada. He moved to Saga University as a Professor in Department of Information Science on April 1990. He was a councilor for the Aeronautics and Space related to the Technology Committee of the Ministry of Science and Technology during from 1998 to 2000. He was a councilor of Saga University for 2002 and 2003. He also was an executive councilor for the Remote Sensing Society of Japan for 2003 to 2005. He is an Adjunct Professor of University of Arizona, USA since 1998. He also is Vice Chairman of the Commission "A" of ICSU/COSPAR since 2008. He wrote 30 books and published 322 journal papers